

Photoswitchable Nanoparticles for Triggered Tissue Penetration and Drug Delivery

Rong Tong,^{†,‡} Houman D. Hemmati,[‡] Robert Langer,[†] Daniel S. Kohane^{*,‡}

[†] Department of Chemical Engineering, Massachusetts Institute of Technology, 77 Massachusetts Avenue, Cambridge, Massachusetts, 02139, United States

[‡] Laboratory for Biomaterials and Drug Delivery, Department of Anesthesiology, Division of Critical Care Medicine, Children's Hospital Boston, Harvard Medical School, 300 Longwood Avenue, Boston, Massachusetts, 02115, United States

EXPERIMENTAL SECTION

General Information. Anhydrous dichloromethane was distilled over CaH₂ and kept anhydrous with 4Å molecular sieves. Docetaxel and doxorubicin·HCl were purchased from LC Laboratories (Woburn, MA) and stored at -20°C in a freezer prior to use. Doxorubicin was desalted using published methods.¹ 2, 3, 3-Trimethyl-3H-indole and lecithin were purchased from Alfa-Aesar (Ward Hill, MA). DSPE-PEG was purchased from Laysan Bio (Arab, AL). Calcein and Cys-Tat(47-57) were purchased from AnaSpec (Fremont, CA). Cy5² and SP derivatives³ were synthesized according to published procedures. All other chemicals were purchased from Sigma-Aldrich (St Louis, MO) and used as received unless otherwise noted. HPLC analysis was performed on a Hewlett Packard/Agilent series 1100 (Agilent, Santa Clara, CA) equipped with an analytical C18 reverse phase column (Kinetex, 75 × 4.6 mm, 2.6 μ, Phenomenex, Torrance, CA). The UV wavelengths for docetaxel, SP, coumarin 6, doxorubicin, rhodamine 6B analysis were set at 227, 350, 350, 450 and 550 nm, respectively. NMR studies were performed on a Varian 500 system (500 MHz). The sizes and polydispersities of NPs were determined on a ZetaPALS dynamic light-scattering (DLS) detector (15 mW laser, incident beam = 676 nm, Brookhaven Instruments, Holtsville, NY). The lyophilization of NPs was carried out on a benchtop lyophilizer (Virtis Benchtop K, SP Scientific, Gardiner, NY). The UV/Vis spectra were recorded with a Varian Cary 50 Bio UV-Visible Spectrophotometer (Agilent, Santa Clara, CA). Flow cytometry was performed on a FACS Calibur (BD bioscience, Bedford, MA) and analyzed by FlowJo (Ashland, OR). Fluorescence microscopy was conducted on an Axiovert 200M Zeiss microscope. UV light for produced with a Dymax Bluewave 75 (Torrington, CT).

Preparation of SP NP_{HS}. DSPE-PEG solution (200 μL, 1 mg/mL in 4 wt% ethanol aqueous solution) was mixed with lecithin (12.5 μL, 1 mg/mL in 4 wt% ethanol aqueous solution) in a vial. SP-C9 in acetonitrile or dimethylformamide (DMF, 400 μL, 1mg/mL) was first mixed with drugs and carefully pipet-

ted into the resulting aqueous solution. Deionized water (3800 μL) was added and the resulting mixture solution was sonicated in a capped glass vial for 5 minutes using a Branson 2510 bath sonicator (Cleveland, OH) at a frequency of 40 kHz and power of 130W. The resulting NP_{HS} were collected after ultrafiltration (5 min, 3000 \times g, Ultracel membrane with 10,000 NMWL, Millipore, Billerica, MA), and washed with water to remove organic solvent. The sizes of NP_{HS} were characterized by DLS.

Lyophilization of SP NP_{HS} in the Presence of Albumin. An aqueous solution of bovine serum albumin (BSA) (12 mg/mL, 500 μL) was added to the SP NP_H solution (1 mg/mL, 400 μL). The mixture was lyophilized for 16 h at -50 $^{\circ}\text{C}$. The resulting white powder was reconstituted with deionized water (2 mL) followed by addition of a concentrated PBS solution (10X, 222 μL). The solution was stirred for 5 min at room temperature. The resulting NC solution was analyzed by DLS.

Determination of Drug (or Dye) Release Kinetics. To determine the release kinetics of SP NP_{HS} loaded with different drugs, a PBS suspension of NPs was placed into Slide-A-Lyzer dialysis tubes (300 μL each tube) with a molecular weight cutoff at 3500 Da (Pierce, Rockford, IL). These microtubes were individually dialyzed in 2 L of PBS buffer (1X) at 37 $^{\circ}\text{C}$. PBS buffer was changed every 24 hours. At scheduled times, NPs solutions from microtubes were collected separately. DMF (300 μL) was added to dissolve the NPs, and the drug/dye content in each tube was measured by HPLC. That content was serially subtracted from the measured starting quantity of drug/dye to determine release kinetics.

Analysis of Cellular Uptake of SP NP_{HS} by Fluorescence Microscope. HeLa cells were grown in chamber slides in DMEM medium (American Type Culture Collection, Manassas, VA), supplemented with 100 units/mL aqueous penicillin G, 100 $\mu\text{g}/\text{mL}$ streptomycin, and 10% FBS (all from Life Technology, Grand Island, NY) at concentrations to allow 70% confluence in 24 h (i.e., 40,000 cells per cm^2). On the day of experimentation, the medium was replaced with Opti-MEM medium (600 μL , Life Technology, Grand Island, NY) containing Cy5/SP NP_{HS} (50 μg). Cells were incubated with NP_{HS} for 2-6 h, and washed with PBS (3 \times 200 μL). Cells in Opti-MEM medium were illuminated by UV light for 1 s and analyzed on the Axiovert 200M Zeiss microscope at 20 \times magnification.

Kinetic Studies. In the dark, the rate of switching from free MC in acetonitrile (or MC NP_{HS}) to SP (or SP NP_{HS}) is given by the previously described equation ⁴ (1) below, where [MC] is the concentration of

free [MC] in acetonitrile or in NP_{HS}; k is the rate constant and t is the time. Integration of equation (1) produces equation (2), where $[MC]_0$ is the initial concentration of MC after UV irradiation.

$$-d[MC]/dt = k[MC] \quad (1)$$

$$\ln([MC]_0/[MC]) = kt \quad (2)$$

The [MC] concentration is directly related to the absorbance A , which can be measured at the λ_{\max} in the UV/Vis spectrum. Equation (3) can be given according to Beer-Lambert law.⁴ A_∞ is the absorbance at infinity at the same wavelength (which is the λ_{\max} of SP NP_H, i.e. the λ_{\max} after MC undergoes complete ring closure to SP-C9); $\Delta\epsilon$ is the difference between molar extinction coefficient of MC and of SP at λ_{\max} ; d is the cuvette's light path length. Combining equations (2) and (3), A could be expressed as a function of t , as shown in equation (4). Fitting a plot of $\ln((A_\infty - A_0)/(A - A_0))$ against t with equation (4) can provide k . $t_{1/2}$ is calculated using equation (2) using the value of k when $[MC] / [MC]_0 = 1/2$.

$$[MC] = (A - A_\infty)/(\Delta\epsilon \cdot d) \quad (3)$$

$$\ln((A_\infty - A_0)/(A - A_0)) = kt \quad (4)$$

Preparation of Cy5/SP NP_M-Cpp Conjugates. DSPE-PEG-maleimide was synthesized following published procedures.⁵ DSPE-PEG / DSPE-PEG-maleimide solution (w/w=9/1, 200 μ L, 1 mg/mL in 4 wt% ethanol aqueous solution) was mixed with lecithin (12.5 μ L, 1 mg/mL in 4 wt% ethanol aqueous solution) in a vial. Cy5 / SP-C9 in DMF (w/w=32.7/400, 400 μ L, 1mg/mL for SP-C9, 5 wt% initial loading wt% for Cy5) was pipetted into the resulting aqueous solution. Deionized water (3787.5 μ L) was added and the resulting mixture was sonicated in a capped glass vial for 5 minutes using a Branson 2510 bath sonicator at a frequency of 40 kHz and power of 130W. The resulting NPs were collected after ultrafiltration (5 min, 3000 \times g, Ultracel membrane with 10,000 NMWL, Millipore, Billerica, MA), and washed with water 3 times to remove DMF and free Cy5 (or other organic solvent). The resulting NPs were reacted with Cys-Tat peptide (Cpp, 1 μ g/ μ L in water, 10 μ L) for 4 hours. The resulting SP NP_M-Cpp was washed with ultrapure water (10 mL) by ultrafiltration (10 min, 1000 \times g, Ultracel membrane with 10,000 NMWL, Millipore, Billerica, MA). The SP NP_M-Cpp were re-suspended (1 mg/mL in deionized water) and applied to cells for fluorescence-activated cell sorting (FACS, BD FACS Calibur's Flow Cytometer) and fluorescence microscopy (Axiovert 200M Zeiss microscope).

Cytotoxicity of SP NP_M-Cpp NPs. HeLa cells were grown in 96-well plates in DMEM medium (Invitrogen, Carlsbad, CA), supplemented with 100 units/ml aqueous penicillin G, 100 µg/mL streptomycin, and 10% FBS at concentrations to allow 70% confluence in 24 h (i.e., 10,000 cells per cm²). On the day of experiments, cells were washed with prewarmed PBS and incubated with prewarmed phenol-red reduced Opti-MEM media for 30 min before the addition of the SP NP_M (50 µg) NPs loaded with doxorubicin (1 wt%) or SP NP_M-Cpp NPs (50 µg, wt% of Cys-Tat) loaded with doxorubicin. The cells were incubated in DMEM medium for 4 h at 37°C, washed with PBS (2× 500 µL per well) and subsequently incubated with DMEM medium for 44 h. The cytotoxicity cells were determined by MTT assay (Sigma-Aldrich, St Louis, MO).

Analysis of cellular uptake of Cy5/NPM-Cpp by FACS. HeLa cells were grown in 6-well plates in DMEM medium (Invitrogen, Carlsbad, CA), supplemented with 100 units/mL aqueous penicillin G, 100 µg/mL streptomycin, and 10% FBS to allow 70% confluence in 24 h (i.e., 40,000 cells per cm²). On the day of experiments, cells were washed with pre-warmed PBS and incubated with pre-warmed phenol-red reduced Opti-MEM media for 30 min before the addition of the NPMs (50 µg) loaded with Cy5 (1 wt%) or Cy5 / SP NPM-Cpp NPs (50 µg, Cy5 % = 1 wt%, ~1 wt% of Cys-Tat). The cells were incubated in DMEM medium for 4 h at 37 °C, washed with PBS (2 × 500 µL per well) and subsequently treated with 0.25% trypsin with EDTA for 10 min (Life Technology, Grand Island, NY). The cells were transferred to a 15 mL centrifuge tube and centrifuged at 1200 rpm for 5 min followed by removal of the trypsin solution. After the cells were washed with PBS (2 × 1 mL), they were fixed with 4% formaldehyde for 10 min at room temperature, washed with PBS (1 × 500 µL) and stored in 1mL PBS with 1 wt% BSA solution at 4 °C for FACS analysis.

Diffusion of ICG/SP NP_{HS} in collagen gels. Collagen hydrogels were prepared by mixing the following components in order on ice: 567 µL of 8.6 mg/mL rat tail collagen I (BD Biosciences, Bedford, MA), 15.2 µL of 1M sodium hydroxide, and 78 µL of 0.17 M EDTA. The final concentration of collagen was 7.38 mg/mL and EDTA was 20 mM. After vortexing, the gel was added to partially fill a microslide capillary tube (Vitrocom, Mountain Lakes, NJ), then incubated for 3 h at 37 °C. 50 µL of ICG/SP NP_{HS} (0.1 mg) solution was placed into the capillary tube with a 30 gauge, in contact with the surface of the collagen gel. The tube was sealed and left at 37 °C for 12 h then imaged by using a near infrared laser scanner (LICOR Odyssey). Image analysis was performed by ImageJ. The fluorescence

intensity (ICG concentration) profile (C) and the distance (x) for the NP_HS before and after irradiation were fitted to the following one-dimensional diffusion model (equation (5))⁶ to obtain the diffusion coefficient D in the collagen gel:

$$C(x, t) = a \cdot \operatorname{erfc} \left(\frac{x}{2\sqrt{t \cdot D}} \right) + b \quad (5)$$

where erfc is the complementary error function and a, b are the constant for the function. The curve was fitted by Origin 8 software (Northampton, MA).

For the calculation of diffusion coefficient in gels of NP_HS that were irradiated by UV twice at different times, the diffusion model was modified to:

$$C(x, t) = a \cdot \operatorname{erfc} \left(\frac{x}{2\sqrt{t_1 \cdot D}} \right) + b \cdot \operatorname{erfc} \left(\frac{x}{2\sqrt{t_2 \cdot D}} \right) + c \quad (6)$$

where a, b, c are the constants for the function, and t_1, t_2 are time intervals after UV treatment (in our case $t_1 = 12\text{h}, t_2 = 9\text{h}$).

***Ex vivo* Topical Administration of Cy5/SP NP_HS in Porcine Cornea Tissues.** Fresh porcine cornea tissues were excised and placed in DMEM medium, supplemented with 100 units/ml aqueous penicillin G, 100 µg/mL streptomycin, and 10% FBS. 1 mg/mL Cy5/SP NP_HS (5 wt% loading of Cy5) was topically administered onto the corneas and incubated for 8 h at 37 °C, with the UV treatment for 1 min ($t=0$). NP_H suspension was then removed and corneas were washed in PBS for 3 times. Tissues were then immediately imaged by a near infrared laser scanner (LICOR Odyssey), then processed for histology (hematoxylin-eosin staining) using standard procedures.

Table S1. SP NPs sizes and stability formulated by nanoprecipitation methods.^[a]

SP/ non-solvent	Size \pm SD ^[a]	PD ^[a]	Size-UV \pm SD ^[a]	PD ^[a]
SP-C9/water	198.1 \pm 2.5	0.09	39.6 \pm 3.0	0.07
SP-C7/water	194.4 \pm 5.2	0.14	239.9 \pm 3.1	0.15
SP-C18/water	184.7 \pm 9.3	0.09	40.4 \pm 1.7	0.06
SP-C9/PBS	Aggr ^[b]	-	-	-
SP-C18/PBS	Aggr ^[b]	-	-	-

^[a] Determined by DLS. Abbreviations: SD: standard deviation; PD: polydispersity; aggr: aggregation; Size-UV: Sizes of NPs treated by UV irradiation. ^[b] The particles aggregated immediately once the aqueous NP solution was added into PBS (N=5).

Table S2. Encapsulation efficiency of SP NPs formulated by nanoprecipitation methods.^[a]

	Initial loading (wt%) ^[a]	Actual loading (wt%) ^[b]	Efficiency% ^[c]
SP-C9 /rhodamine B	5	0.35 ± 0.09	7.09
SP-C9 / coumarin 6	5	0.51 ± 0.05	10.12
SP-C18 / rhodamine B	5	0.53 ± 0.03	10.51
SP-C18 /coumarin 6	5	0.64 ± 0.03	12.82

^[a] Theoretical, based on materials used.

^[b] Determined by HPLC (N=5).

^[c] Efficiency % = Actual loading / Initial loading × 100.

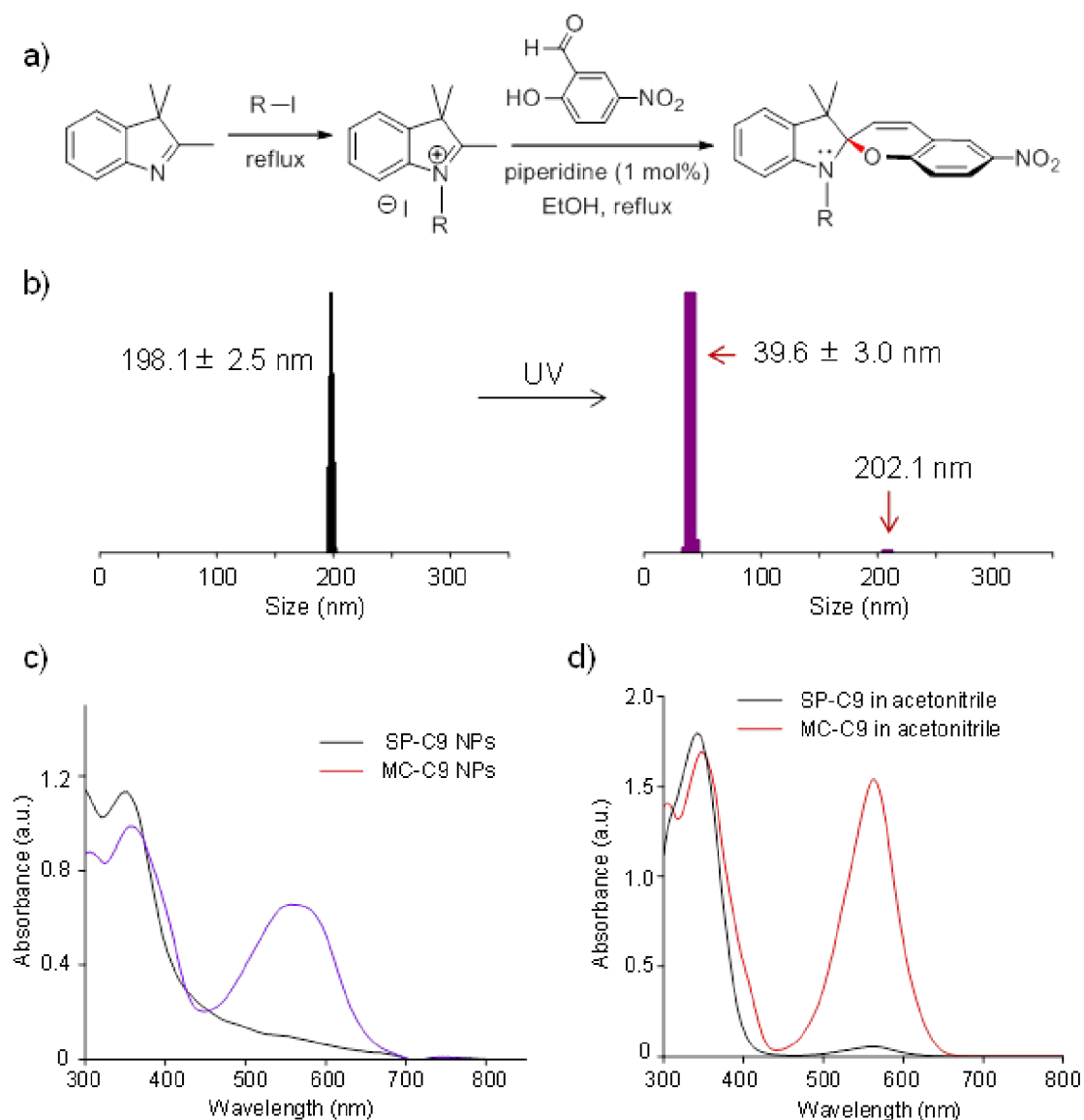


Figure S1. (a) Scheme of SP synthesis. (b) Dynamic light scattering measurement of size changes of SP-C9 NPs upon UV illumination (30s). (c) Steady-state absorption spectra of SP-C9 NPs ($[SP-C9] = 0.46 \text{ mM}$, black line) and corresponding isomerized MC-C9 NPs ($\lambda_{\text{max}} = 551 \text{ nm}$, purple line) after UV light irradiation. (d) Steady-state absorption spectra of free SP-C9 in acetonitrile ($[SP-C9] = 0.46 \text{ mM}$, black line) and its corresponding isomerized MC-C9 ($\lambda_{\text{max}} = 560 \text{ nm}$, purple line) after UV light irradiation.

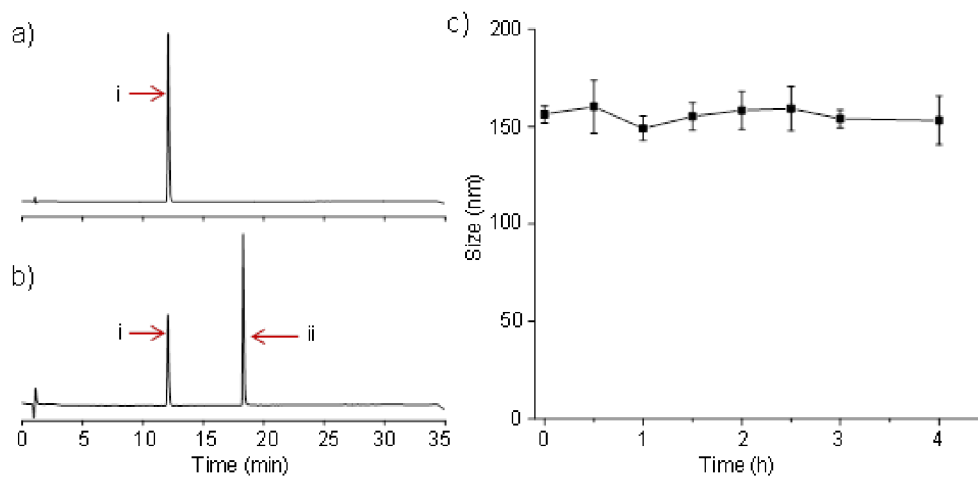


Figure S2. SP NP_H encapsulating coumarin 6 (initial loading wt% =10%). a, b) HPLC analysis with the UV detector wavelength set at 360 nm. (The maximum absorbance of coumarin 6 and SP-C9 are both around 360 nm.) a) Filtrate solution after washing of NP_H by ultracentrifugation. b) NP_H dissolved in DMSO after washing. Peak labels: i: coumarin 6; ii: SP-C9. (c) Stability of NP_Hs in PBS over time. Data are means \pm SD. N=5.

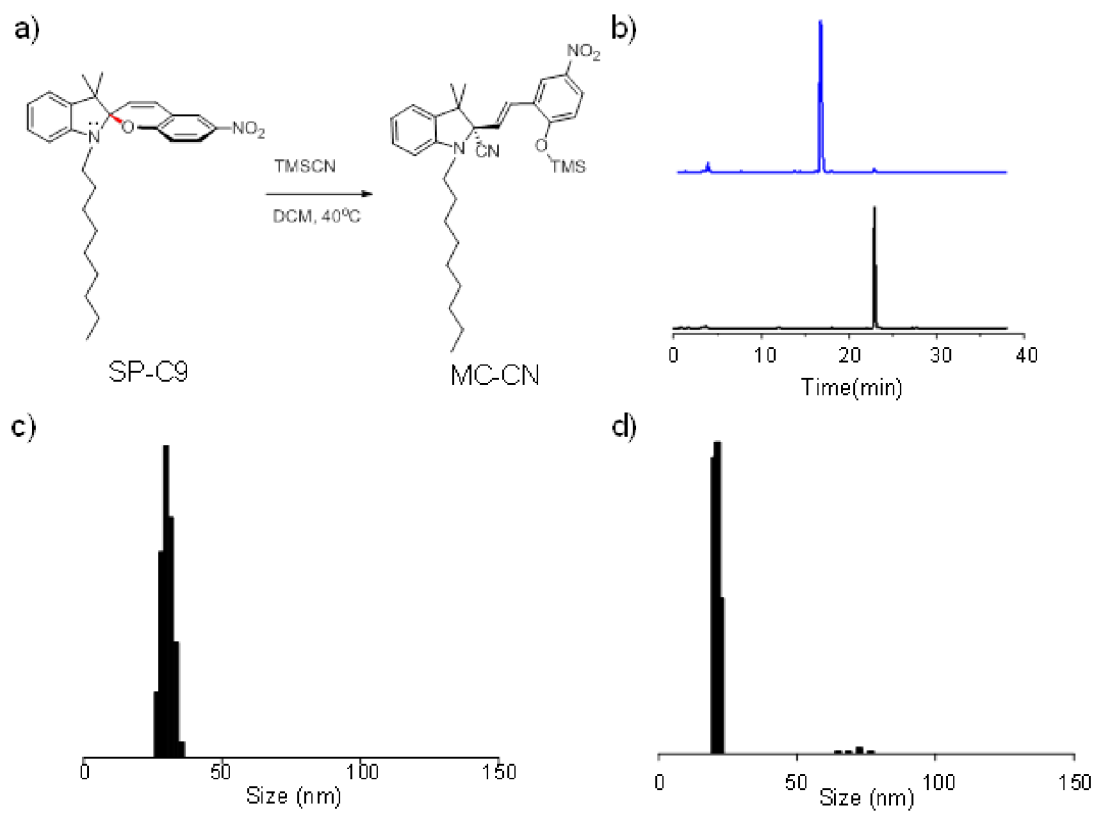


Figure S3. (a) Scheme of MC-CN synthesis by the 1,6 addition of SP-C9 and MC-CN; (b) analytical HPLC traces of SP-C9 (black line) and MC-CN (blue line). Size number distributions of (c) MC-CN NP_H and (d) MC-CN NPs (no lipids or PEG), determined by dynamic light scattering

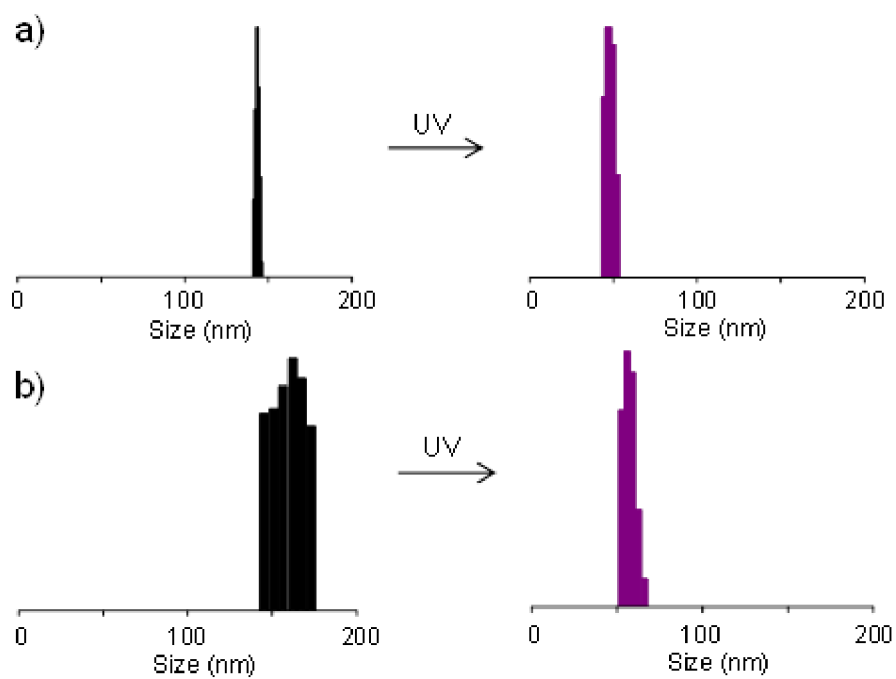


Figure S4. Size switching upon UV irradiation of SP NP_H. (a) before lyophilization; (b) after lyophilization with bovine serum albumin (BSA) and storage at -20 °C for over one month (N=4).

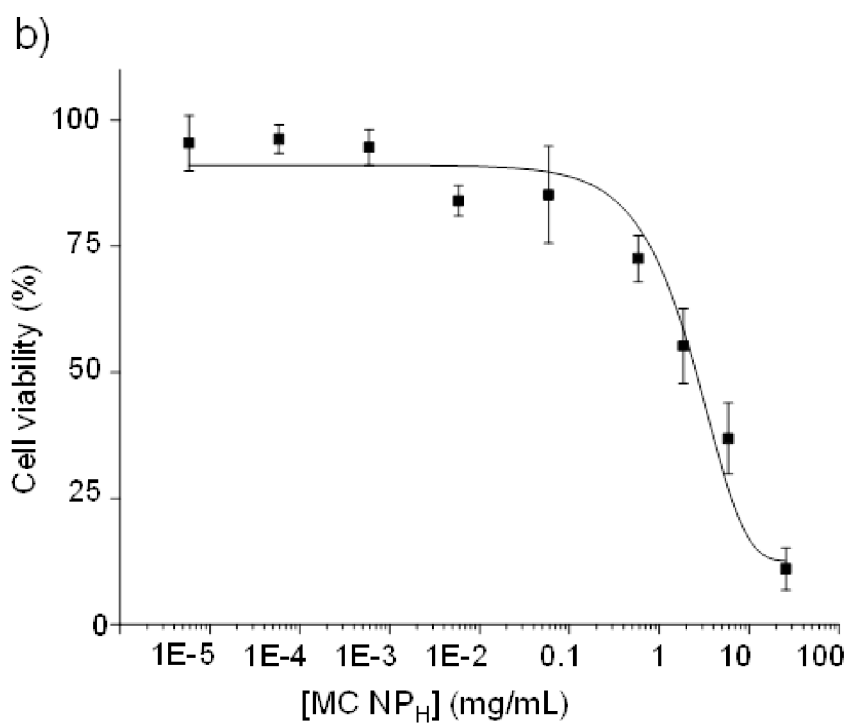
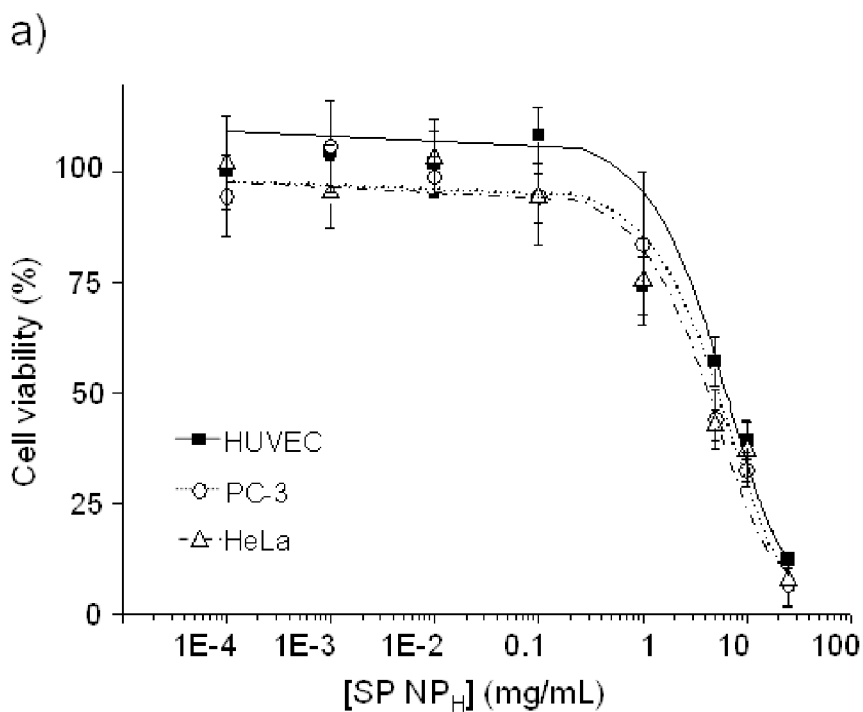


Figure S5. MTT cytotoxicity assays for NP_H. (a) Cytotoxicity of SP NP_Hs in HUVEC, PC-3 and HeLa cells. (b) Cytotoxicity of MC NP_H in HeLa cells. The MC NP_H were prepared by UV irradiation for 5-20 s to ensure complete formation of MC prior to cell culture and repeated irradiation at 3h and 6h for 2s while in culture. All NPs were incubated with cells at 37°C for 72 hours. Data are means ± SD, N=6).

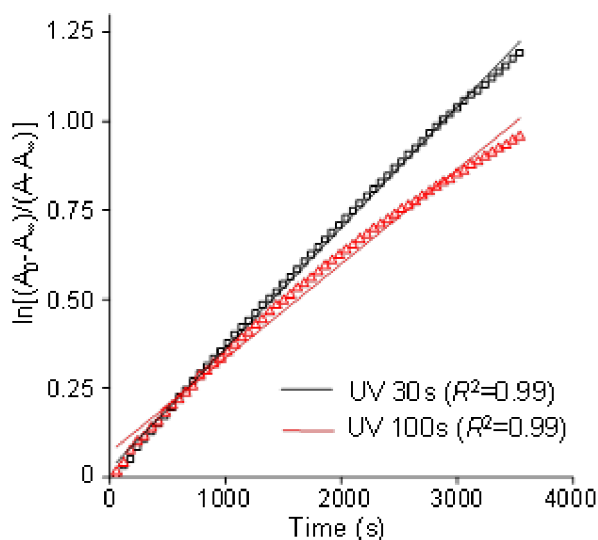


Figure S6. The kinetics of ring-closing reactions of MC NP_H upon UV illumination for 30s (black) and 100 s (red). A₀: Initial MC absorbance after UV illumination. A_∞: absorbance at infinity, which is the the λ_{max} of SP NP_H, i.e. after MC undergoes complete ring closure to SP-C9).

Discussion:

For SP derivatives, both O₂-dependent and O₂-independent mechanisms have been identified for photo-fatigue (also termed photo-degradation; detailed mechanism is discussed in Scheme S1).⁷ In figure S6, the absorption intensity of MC in NP_H at 551 nm faded at a rate dependent on the duration of UV (365 nm) irradiation which is consistent with an O₂-independent fatigue mechanism for SP.⁸ Furthermore, addition of antioxidant agents (e.g. 4-methoxy-1, 2, 2, 6, 6-pentamethylpiperidine and 4-methoxy-2, 2, 6, 6-tetramethylpiperidine)^{7b} to SP NP_Hs in a 10-fold molar excess to SP could not eliminate photo-fatigue of NPs, suggesting that O₂-dependent photo-fatigue is not the mechanism. These studies suggest that O₂-independent mechanisms caused the decrease in absorption by MC at λ_{max} and the alterations in SP NP_H sizes after repetitive UV/Vis triggering.

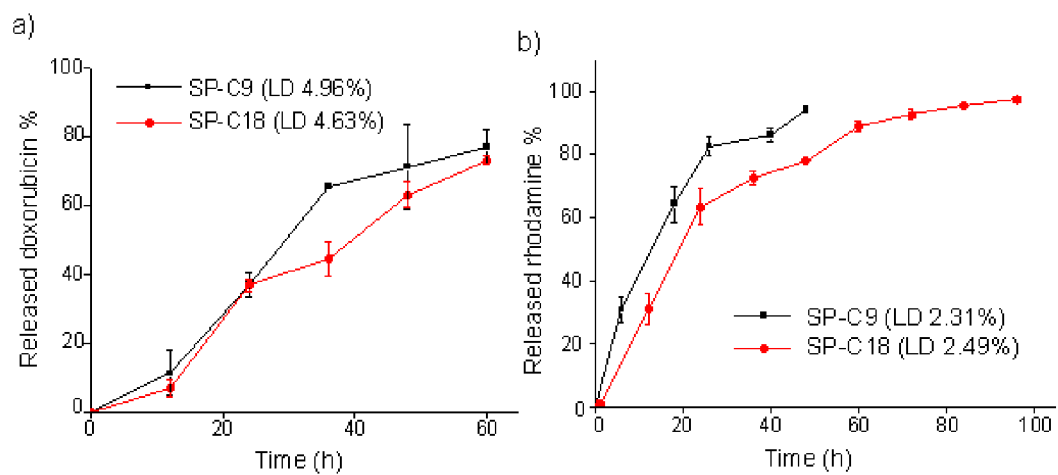


Figure S7. The release profiles of (a) Doxorubicin from SP-C9 and SP-C18 NP_H; and (b) Rhodamine B from SP-C9 and SP-C18 NP_H. LD: loading. Data are means \pm SD, N=6

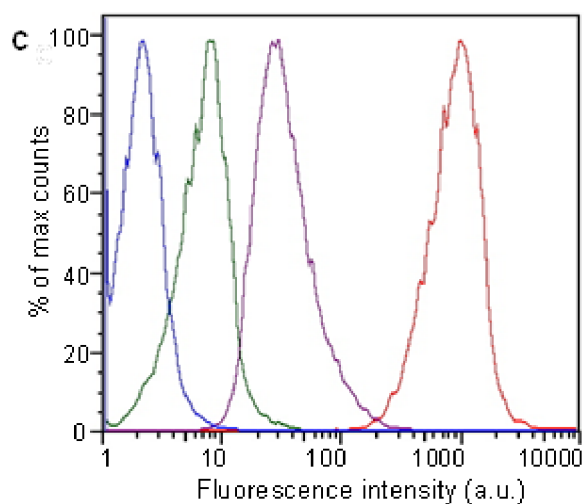
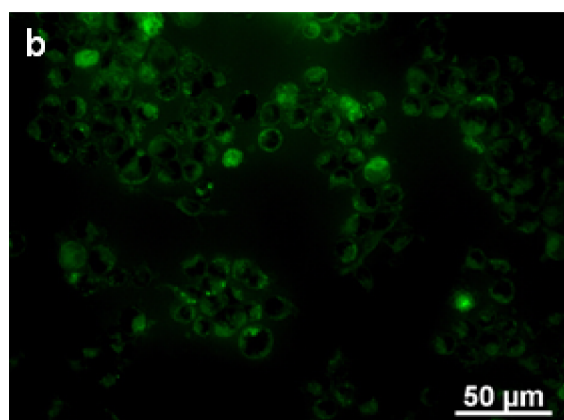
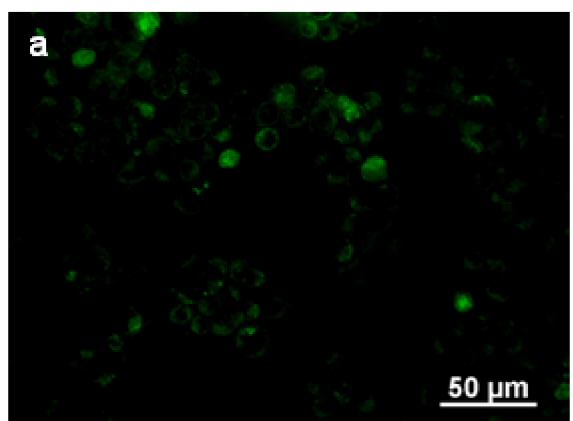


Figure S8. UV-triggered release of calcein (green fluorescence) from SP NP_H (calcein loading wt% = 2.7 wt%). Cells were incubated for 4 hrs with calcein-containing NP_H then washed with PBS. Cells were then irradiated with UV for 2s every 5 minutes, and an image was captured 5 minutes after each UV illumination. The fluorescence intensity in HeLa cells gradually increased from (a, before irradiation) to (b, after 4 cycles of irradiation). (c) Flow cytometry. HeLa cells were incubated with calcein-containing SP NP_H for 4 hrs as in (a). Flow cytometric analysis of green fluorescence intensity was then performed for cells without (purple line) or with UV illumination (10 s, red line). HeLa cells exposed to NPs containing no dye (green line) and cells without SP NP_H or dyes (blue line) were assayed for comparison. (Wavelengths for excitation and emission were 480 nm and 510 nm, respectively.)

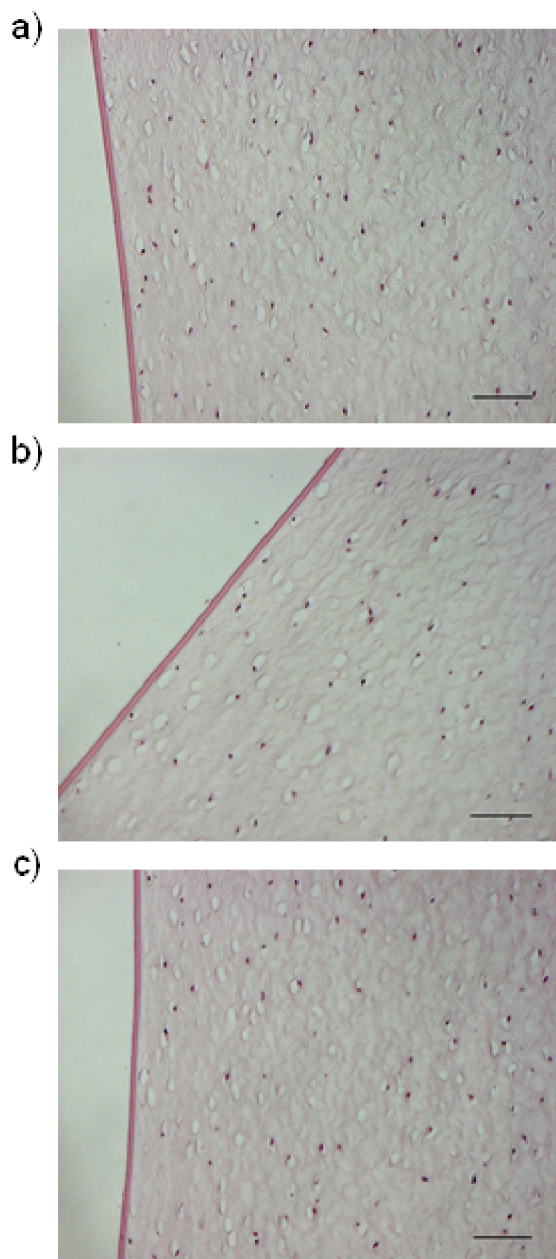


Figure S9. Hematoxylin-eosin stained sections of (a) corneas incubated in DMEM without any treatment; (b) corneas treated with Cy5/SP NP_H triggered by UV light for 1 min; (c) corneal tissues incubated with Cy5/SP NP_H. All incubations were for 8 hours. The scale bar = 50 μm.

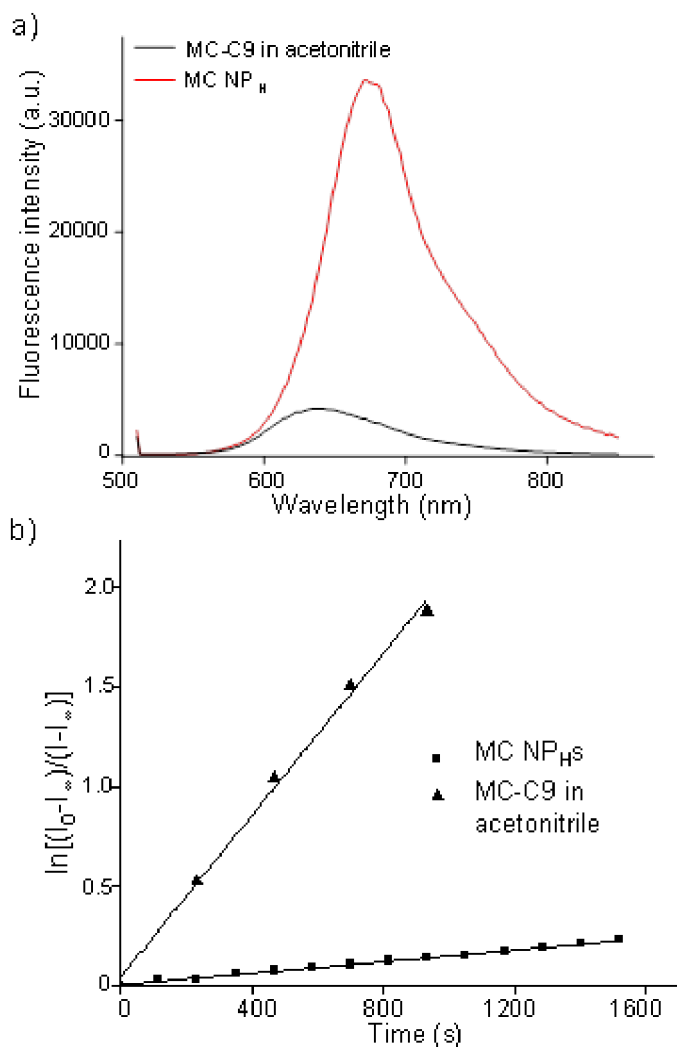


Figure S10. (a) Fluorescence emission spectra of MC-C9 in acetonitrile (black curve) and of MC NP_H (red curve); both are measured immediately after 30s UV irradiation. The MC concentration was 0.43 mM in both cases. Excitation wavelength: 480 nm. The λ_{\max} for MC NP_H and free MC in acetonitrile were 672 and 640 nm, respectively. (b) Representative exponential decay kinetics of fluorescence intensity of MC NP_H and MC-C9 in acetonitrile (N=5). I_0 : Initial MC-C9 fluorescence intensity after UV illumination. I_∞ : fluorescence intensity at infinity, which is the absorbance value of SP NP_H at the λ_{\max} of MC NP_H after MC-C9 reverts to SP-C9.

Discussion:

The red-shift of the λ_{\max} of MC in MC NP_H from 640 nm to 672 nm (Figure S10a) reflects the assembly state of MC in NPs. The tendency of free SP/MC to undergo aggregation in organic membranes and films is well known⁹. Three types of aromatic dye aggregates have been described: dimers, H-aggregates, and J-aggregates.¹⁰ The spectra of dimers and H-aggregates are blue-shifted relative to the molecularly dispersed monomers, whereas J-aggregates are red-shifted in fluorescence spectrum.^{10b,11} Therefore, it is likely that MC-C9 forms J-aggregates inside NP_H (see Scheme S2 and Figure 9).

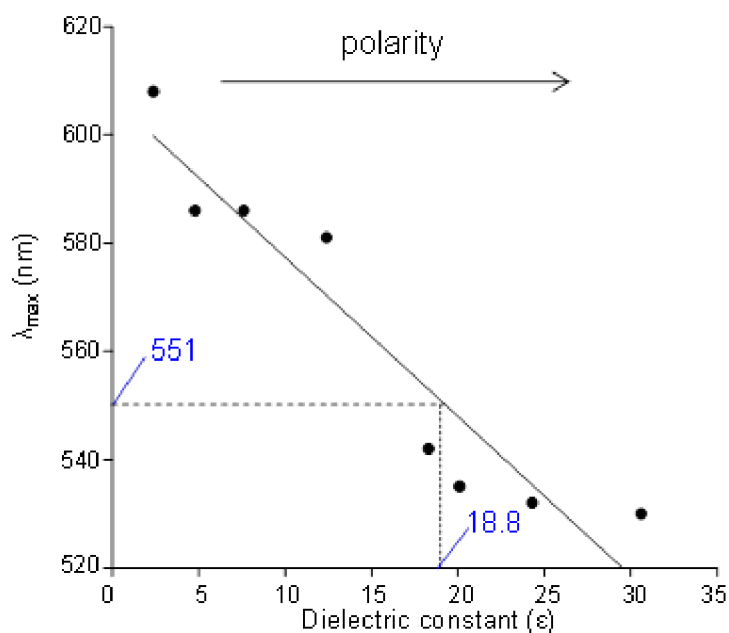


Figure S11. Effect of the solvent dielectric constant (ϵ) on the spectrum maximum (λ_{\max}) of MC. The solvents used (with ϵ in parentheses) were toluene (2.38), chloroform (4.8), tetrahydrofuran (7.6), dichloromethane (9.08), pyridine (12.4), 2-propanol (18.3), 1-propanol (20.1), ethanol (24.3), and methanol (32.6). The solid line is the best linear fit to the data points. The dashed horizontal line corresponds to the λ_{\max} of MC NP_H.

Discussion:

The λ_{\max} of MC is sensitive to its solvent or microenvironment, a property termed solvatochromism: the λ_{\max} of MC shifts to higher energy (lower wavelength in spectrum) as the polarity of the solvent or microenvironment increases.¹² Here we studied the relationship between the dielectric constant (ϵ), an indicator of the polarity of the solvent, and the λ_{\max} of the MC in order to make inferences about the microenvironment of MC^{10b,12-13} in the NP_H.

To elucidate the relationship between microenvironment polarity ϵ and λ_{\max} , we plotted the λ_{\max} of MC-C9 in organic solvents with various ϵ .^{10b,12} Extrapolation of the λ_{\max} value (551 nm) for MC NP_H to the abscissa (dashed line in Figure S11) suggested an effective ϵ around 18, which is comparable to the λ_{\max} measured in a relatively polar solvent (for isopropanol $\epsilon = 18.3$, $\lambda_{\max} = 542$ nm). These findings indicated that MC-C9 molecules are likely located in relative polar microenvironments in the MC NP_H. Previous studies of MC derivatives in liposomes suggest that MC-C9 might localize near the phosphoglycerol moiety linking PEG and DSPE.^{10b,13}

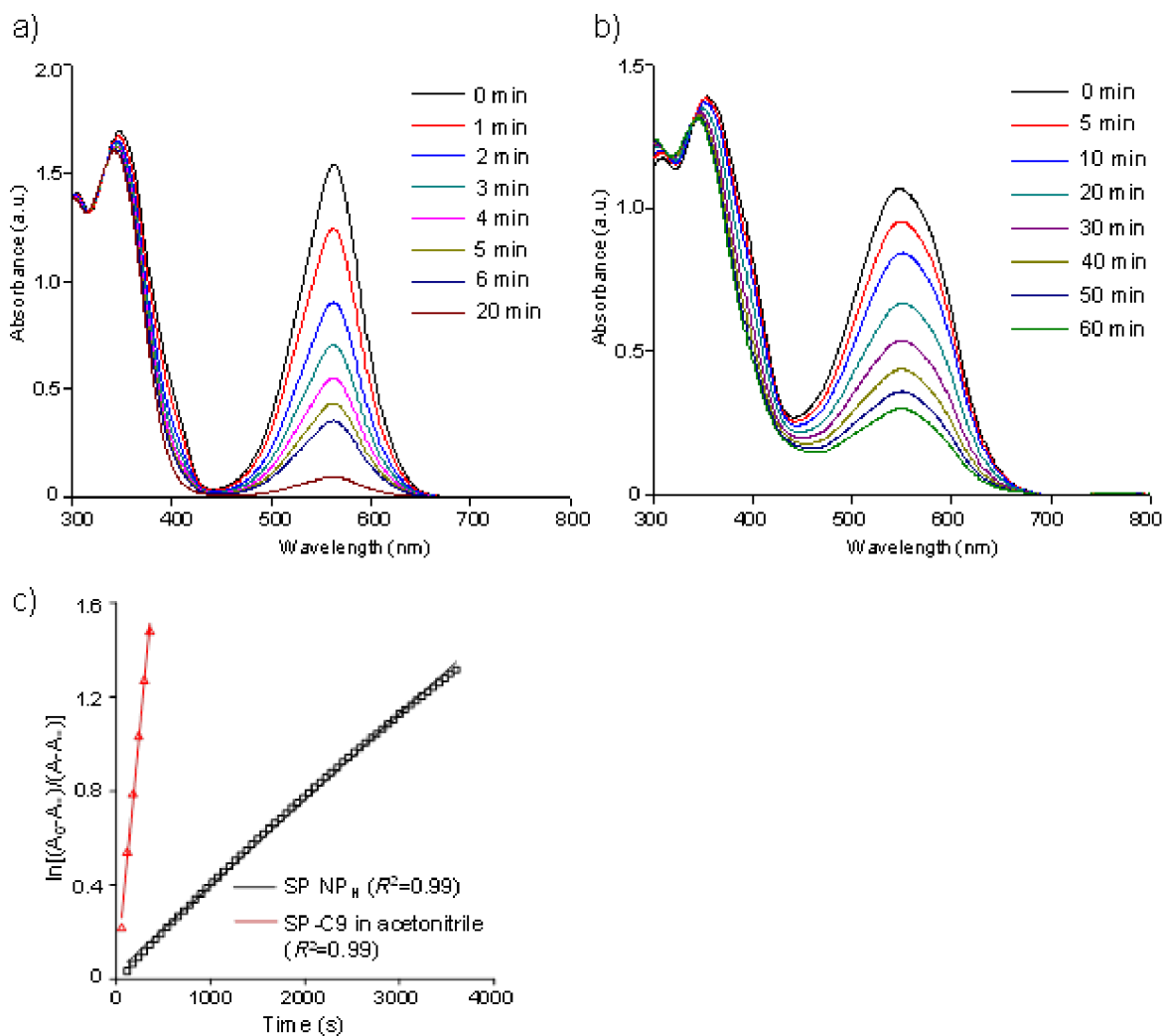
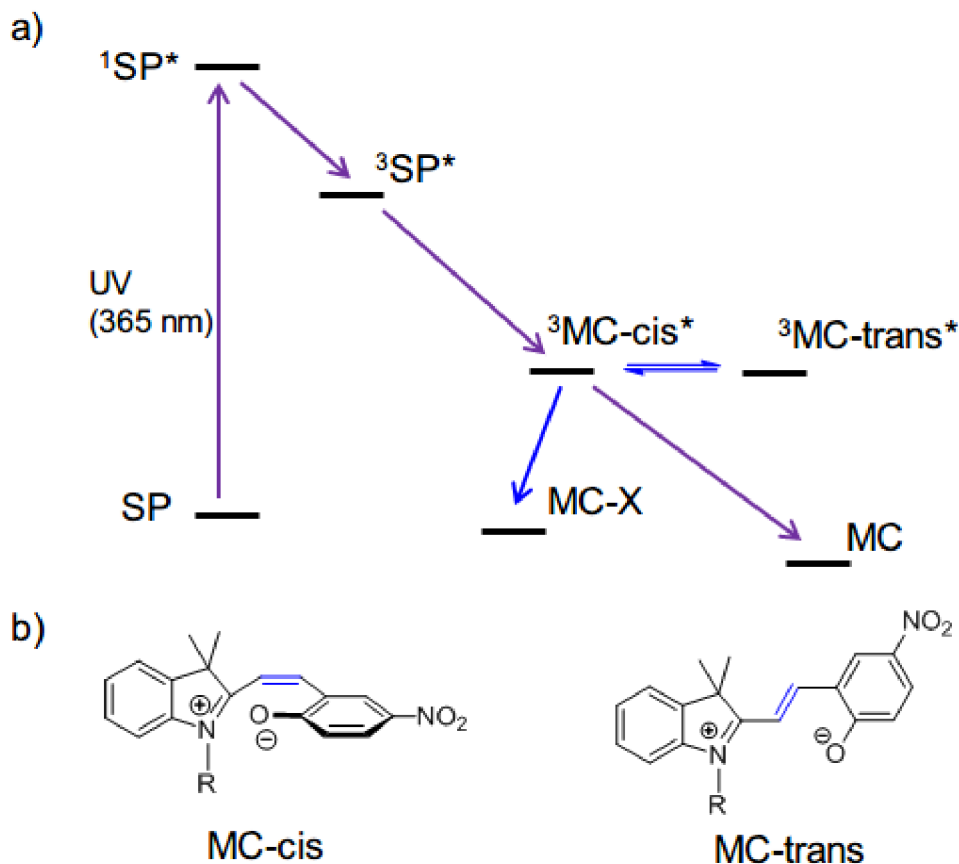


Figure S12. Representative UV/Vis absorption spectra of the isomerization of MC to SP, either in (a) acetonitrile solution or in (b) NP_H. MC was generated by prior UV irradiation (30s) and the reversion of MC to SP occurred in the dark (N=4). ([MC-C9] = 0.46 mM in both acetonitrile and NP_H). (c) The first-order kinetics of the isomerization of MC to SP at λ_{\max} of panels (a) (at 560 nm, red) and (b) (at 551 nm, black).

Discussion:

The UV-triggered conversion of SP NP_H to MC NP_H showed an exponential increase in the absorbance at λ_{\max} of MC (551 nm) at a rate constant (k^1) of $0.064 \pm 0.016 \text{ s}^{-1}$ ($t_{1/2} = 14.8 \pm 3.7 \text{ s}$, N=4, [SP-C9] = 0.69 mM, primary data not shown) for the ring-opening reaction of SP to MC. Subsequently, the isomerization of MC to SP occurred slowly in the dark, which in MC NP_H followed first-order decay with a rate constant (k^1) of $3.66 \pm 0.13 \times 10^{-4} \text{ s}^{-1}$ at $\lambda_{\max}=551 \text{ nm}$ (N=4, $t_{1/2} = 1732 \pm 70 \text{ s}$). This rate of MC conversion to SP in NP_H was 12.2-fold slower than that of free MC in acetonitrile (N=4, $k^1 = 4.46 \pm 0.07 \times 10^{-3} \text{ s}^{-1}$ at $\lambda_{\max}=560 \text{ nm}$, $t_{1/2} = 155 \pm 2 \text{ s}$). The slowness of the isomerization of MC to SP in NP_H (compared to in acetonitrile) is likely due to microenvironmental restriction of MC's conformational change to SP. A similar phenomenon has been observed in SP embedded in polymeric films.^{8a}

Scheme S1. (a) Reported photo-processes of SP derivatives.^{7e,14} The ring-opening pathway is depicted by purple arrows. Side reactions are depicted by blue arrows. ‘*’ represents a vibrationally excited state. ‘¹SP*’ represents the singlet excitation state and ‘³SP*’ represents the triplet excitation state. ‘MC-X’ represents unknown isomers and pathways that MC-cis relaxes to, as indicated by references.¹ ‘MC-cis’ and ‘MC-trans’ represent the *cis* and *trans* isomers of MC, as shown in (b). The side reaction from the triplet state ‘³MC-Cis*’ to ‘MC-X’ causes photo-fatigue effects and undesired side products in the photo-process.



Discussion:

The O₂-independent mechanism has been reported to be dominant in SP,^{7e,14} with photo-degradation occurring primarily from the triplet manifold. After UV triggering, around 90% of UV-irradiated SP derivatives will be in the excited singlet SP state and will further transform to corresponding MC isomers. Approximately 10% will proceed through a triplet state with little probability of forming MCs, leading to fatigue.¹⁵ The probability of O₂-independent fatigue is reported to be related to the UV irradiation time,^{8b,15} which is also observed in our experiments (Figure S6).

References

- (1) Tong, R.; Cheng, J. J. *J. Am. Chem. Soc.* **2009**, *131*, 4744.
- (2) Shmanai, V. V.; Kvach, M. V.; Ustinov, A. V.; Stepanova, I. A.; Malakhov, A. D.; Skorobogatyi, M. V.; Korshun, V. A. *Eur. J. Org. Chem.* **2008**, 2107.
- (3) Buncel, E.; Wojtyk, J. T. C.; Kazmaier, P. M. *Chem. Mater.* **2001**, *13*, 2547.
- (4) Raymo, F. M.; Giordani, S. *J. Am. Chem. Soc.* **2001**, *123*, 4651.
- (5) Kirpotin, D.; Park, J. W.; Hong, K.; Zalipsky, S.; Li, W. L.; Carter, P.; Benz, C. C.; Papahadjopoulos, D. *Biochemistry-Us* **1997**, *36*, 66.
- (6) (a) Clauss, M. A.; Jain, R. K. *Cancer Res.* **1990**, *50*, 3487; (b) Ramanujan, S.; Pluen, A.; McKee, T. D.; Brown, E. B.; Boucher, Y.; Jain, R. K. *Biophys J* **2002**, *83*, 1650; (c) Wong, C.; Stylianopoulos, T.; Cui, J. A.; Martin, J.; Chauhan, V. P.; Jiang, W.; Popovic, Z.; Jain, R. K.; Bawendi, M. G.; Fukumura, D. *Proc. Natl. Acad. Sci. U. S. A.* **2011**, *108*, 2426.
- (7) (a) Minkin, V. I. *Chem. Rev.* **2004**, *104*, 2751; (b) Li, X. L.; Li, J. L.; Wang, Y. M.; Matsuura, T.; Meng, J. B. *Journal of Photochemistry and Photobiology a-Chemistry* **2004**, *161*, 201; (c) Baillet, G.; Giusti, G.; Guglielmetti, R. *Journal of Photochemistry and Photobiology a-Chemistry* **1993**, *70*, 157; (d) Baillet, G.; Campredon, M.; Guglielmetti, R.; Giusti, G.; Aubert, C. *Journal of Photochemistry and Photobiology a-Chemistry* **1994**, *83*, 147; (e) Matsushima, R.; Nishiyama, M.; Doi, M. *Journal of Photochemistry and Photobiology a-Chemistry* **2001**, *139*, 63.
- (8) (a) Tamai, N.; Miyasaka, H. *Chem. Rev.* **2000**, *100*, 1875; (b) Zhu, L. Y.; Zhu, M. Q.; Hurst, J. K.; Li, A. D. Q. *J. Am. Chem. Soc.* **2005**, *127*, 8968.
- (9) Seki, T.; Ichimura, K. *J Phys Chem-Us* **1990**, *94*, 3769.
- (10) (a) Kasha, M.; Rawls, H. R.; Ashraf El-Bayoumi, M. *Pure Appl. Chem.* **1965**, *11*, 371; (b) Khairutdinov, R. F.; Giertz, K.; Hurst, J. K.; Voloshina, E. N.; Voloshin, N. A.; Minkin, V. I. *J. Am. Chem. Soc.* **1998**, *120*, 12707.
- (11) Würthner, F.; Kaiser, T. E.; Saha-Möller, C. R. *Angewandte Chemie International Edition* **2011**, *50*, 3376.
- (12) Khairutdinov, R. F.; Hurst, J. K. *Langmuir* **2001**, *17*, 6881.
- (13) Mazeret, S.; Schram, V.; Tocanne, J. F.; Lopez, A. *Biophys J* **1996**, *71*, 327.
- (14) Buback, J.; Kullmann, M.; Langhojer, F.; Nuernberger, P.; Schmidt, R.; Wurthner, F.; Brixner, T. *J. Am. Chem. Soc.* **2010**, *132*, 16510.
- (15) Sakuragi, M.; Aoki, K.; Tamaki, T.; Ichimura, K. *B Chem Soc Jpn* **1990**, *63*, 74.